GEOLOGICAL SURVEY OF CANADA
OPEN FILE 7324

Strong Motion Data from the Magnitude 7.7 "Haida Gwaii" Earthquake on October 27, 2012 (local time)

A. Rosenberger, A. Bird, M.E. Turek, S. Huffman, G. Rogers, J. Cassidy, T. Mulder

2013

Natural Resources Canada | Ressources naturelles Canada

Canada

GEOLOGICAL SURVEY OF CANADA
OPEN FILE 7324

Strong Motion Data from the Magnitude 7.7 "Haida Gwaii" Earthquake on October 27, 2012 (local time)

A. Rosenberger[2], A. Bird[2], M.E. Turek[1], S. Huffman[1], G. Rogers[2], J. Cassidy[2], T. Mulder[2]

[1] Ministry of Transportation and Infrastructure BC, 940 Blanchard St., Victoria, BC, Canada,V8W 3E6
[2] Geological Survey of Canada, Pacific Geoscience Centre, 9860 W. Saanich Rd., Sidney, BC, Canada, V8L 4B2

2013

©Her Majesty the Queen in Right of Canada 2013

doi:10.4095/292275

This publication is available for free download through GEOSCAN (http://geoscan.ess.nrcan.gc.ca/).

Recommended citation
Rosenberger, A., Bird, A., Turek, M.E., Huffman, S., Rogers, G., Cassidy, J., and Mulder, T., 2013. Strong Motion Data from the Magnitude 7.7 "Haida Gwaii" Earthquake on October 27, 2012 (local time); Geological Survey of Canada, Open File 7324, 34 p. doi:10.4095/292275

Publications in this series have not been edited; they are released as submitted by the author.

Contents

1 Introduction

On October 27, 2012 at 8:04 p.m. local time (Oct. 28, 03:04 UTC) a magnitude 7.7 (Mw) earthquake with a predominantly thrust mechanism occurred off southern Moresby Island in Haida Gwaii, British Columbia The hypocentre was near 52.3 latitude and -132.3 longitude, about 80km south-west of Queen Charlotte City with a depth of about 19 km, but the seismogenic rupture surface extends both northwest and southeast, mainly to the southeast, with total length of about 100 km.

We present a preliminary analysis of strong motion data from the British Columbia strong motion network (Rosenberger et al., 2006) for the main shock and one of the larger aftershocks (Mw 6.3, -132.8°, 52.5°, depth 20km, 2012-10-28, 18:54 UTC).

Three instruments, recently added to the network by the Ministry of Transportation and Infrastructure BC (MoT-I BC) to be part of the BC Smart Infrastructure Monitoring System (BCSIMS, Ventura et al. (2012)), have recorded ground motions from the events (see Fig. 1).

Location	Station code	Lat	Lon
Masset	MSS01	54.022	-132.1578
Queen Charlotte City	QCC01	53.2556	-132.0837
Prince Rupert	PRP01	54.3038	-130.3356

2 Tectonic setting

The Queen Charlotte Fault (QCF) runs along the boundary between the Pacific and North American Plates, adjacent to the west coast of Haida Gwaii, and has recorded many large earthquakes in the past, including a magnitude 8.1 in 1949. The boundary is dominantly transform (strike-slip), although there is a definite element of compression adjacent to Moresby Island, as the fault curves further eastward along this section, causing the relative Pacific - North American motion to become transpressional.

Evidence so far suggests that the magnitude 7.7 earthquake that occurred on October 28th (UTC) had a very complicated rupture with most of the rupture surface on a low angle thrust fault just west of the surface trace of the QCF fault. This is different from the predominantly strike-slip motion that occurs along along the QCF. Aftershocks continue with great frequency and varying focal mechanisms. Most aftershocks have had magnitudes generally below 5.5 but there has been one magnitude 6.3 and one magnitude 6.2 thus far. The M7.7 is the largest earthquake to hit Canada since 1949 and is of great interest to the seismological research community.

3 Data processing

The acceleration time series are corrected for bias, by computing the mean acceleration value for each channel over the time window and subtracting this value from the each sample.

Before integration to velocity, the acceleration time series from each channel are windowed with a cosine roll-on/roll-off taper. Roll-on and roll-of time is 30 seconds. Subsequently data are high-pass filtered with a third order causal butterworth filter with 0.1Hz cut-off. The same processing is applied before integrating velocity to displacement. Spectral acceleration response is calculated with 5% damping.

Peak acceleration values for the main shock for the three sites, together with predicted values from the ground motion prediction equations (GMPE) of Atkinson and Boore (2003) and Boore and Atkinson (2008), are summarized in figure 2. This earthquake is in a subduction like setting so Atkinson and Boore (2003) may be the more appropriate GMPE for comparison. We have used the closest approach to the area of concentrated aftershock activity to calculate the distance of the respective instrument from the presumed fault zone.

Time series of acceleration, velocity and displacement for the Queen Charlotte City and Prince Rupert sites are shown for both events, the 7.7 main shock of October 28, 3:04 UTC and the Mw 6.3 aftershock of October 28, 18:54 UTC, on the following pages. The October 28 aftershock was also recorded by the Masset instrument but the recording is severely compromised from an interfering signal of yet unknown origin. Only the acceleration time series is presented.

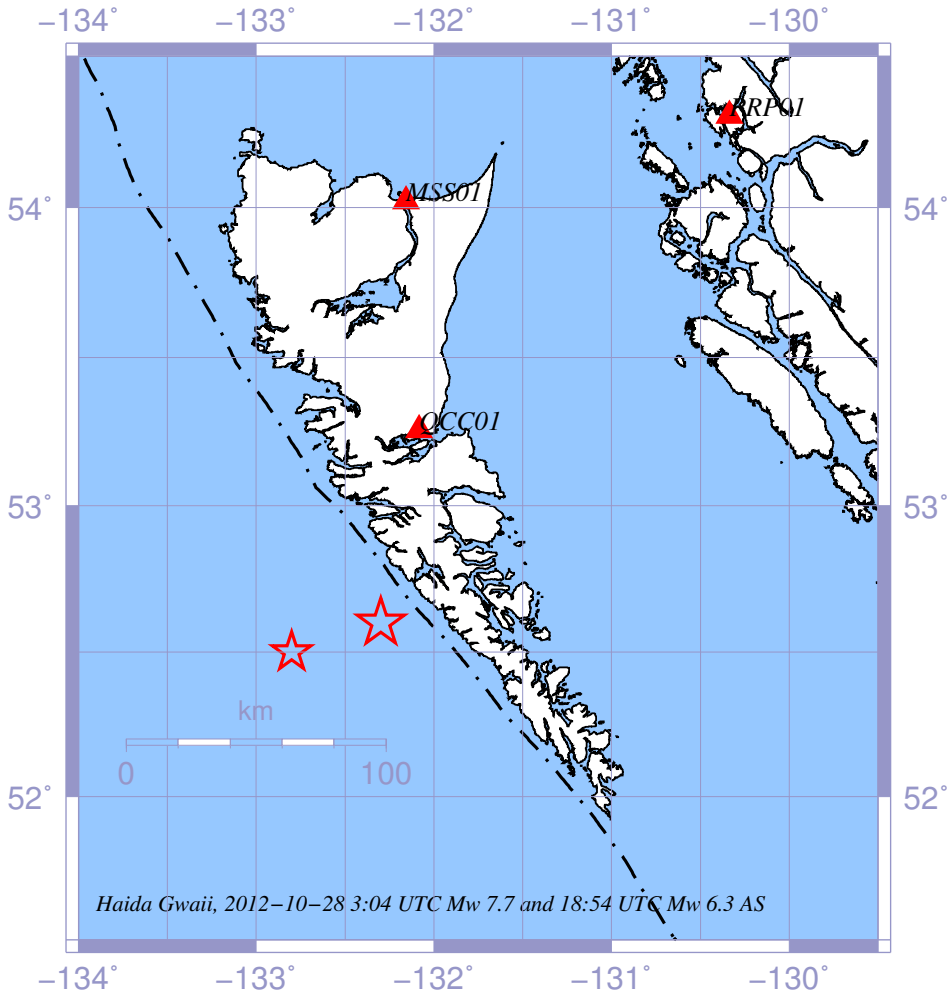

Figure 1: The epicentres of the Mw 7.7 main shock and the Mw 6.3 after-shock of 2012-10-28, 18:54 UTC. The rupture is bilateral with the rupture surface extending to the northwest and southeast of the epicentre. Strong motion stations QCC01 and PRP01 have recorded both events. The after-shock recording of MSS01 suffers from mechanical or electro-magnetic interference.

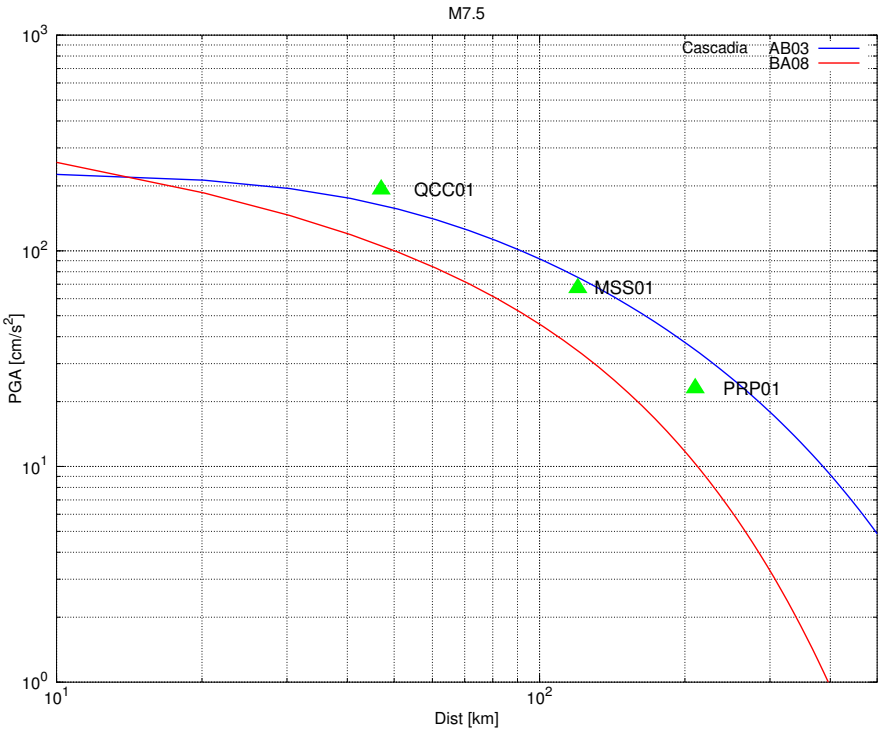

AB03: Atkinson, Boore, BSSA 93.4, 2003
BA08: Boore, Atkinson, EQ Spectra, 24.1, 2008

Figure 2: Recorded peak ground acceleration (PGA) from the Haida Gwaii and Prince Rupert instruments. Distance is calculated from the closest approach to the area of concentrated after-shock activity (assumed to be at $52.97°, -132.6°$). For comparison the attenuation curves based on ground motion prediction equations from Atkinson and Boore (2003) and Boore and Atkinson (2008) are shown.

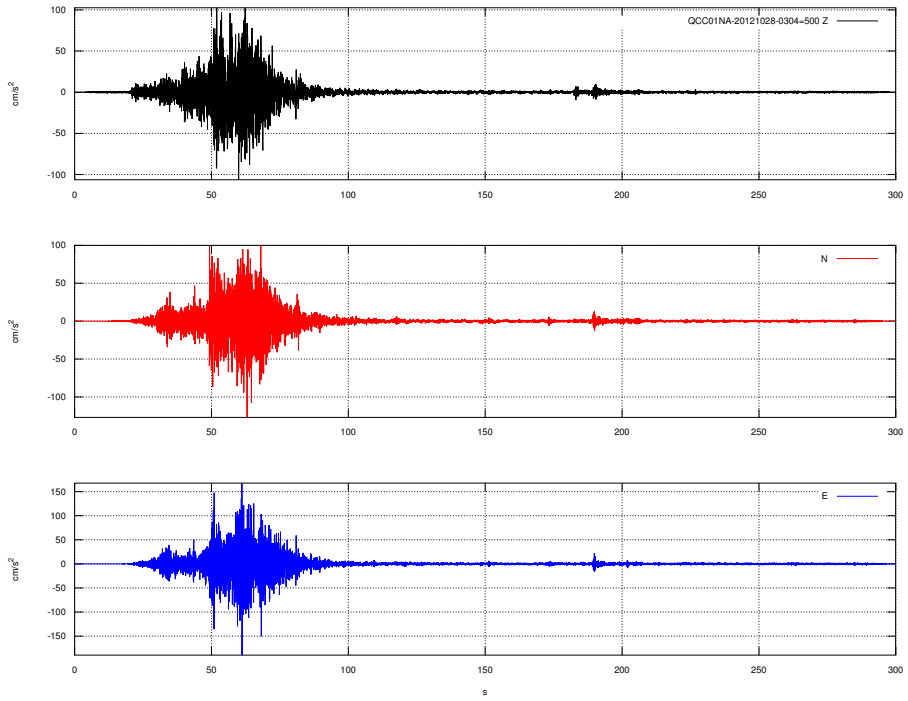

Figure 3: QCC01, main event, acceleration record. Time axis starts at 3:04:30 UTC. Scale is different on all plots, peak ground acceleration of $192 cm/s^2$ occurs at about 60 s on the E-W component.

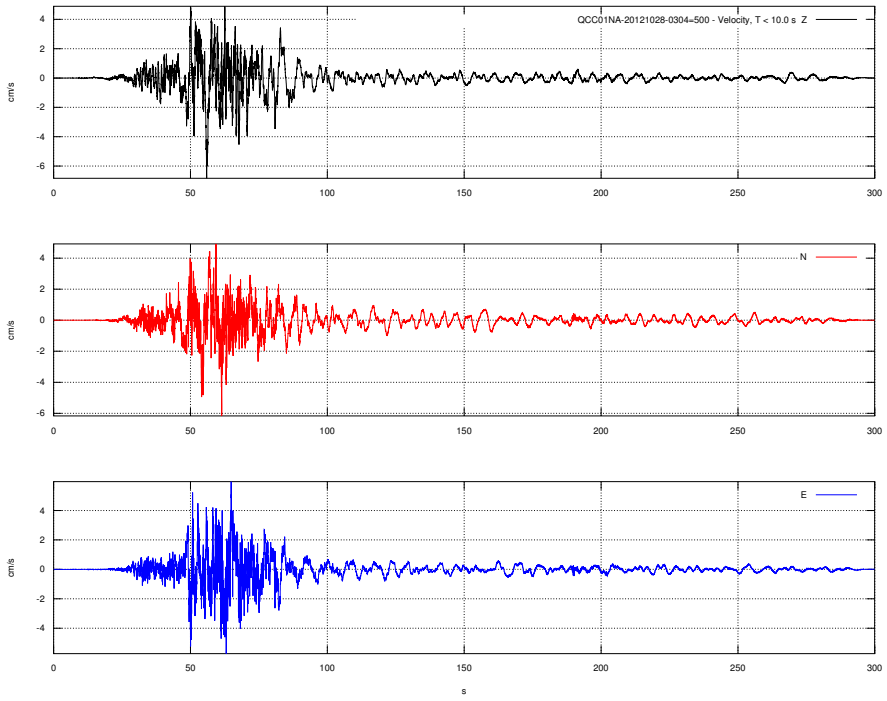

Figure 4: QCC01, main event, velocity record. Time axis starts at 3:04:30 UTC.

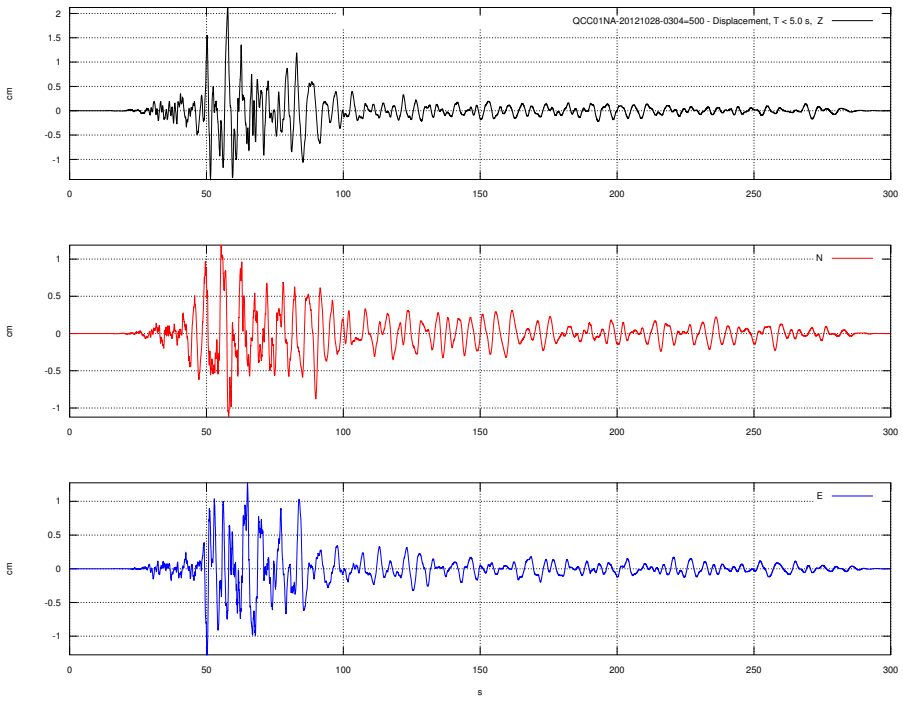

Figure 5: QCC01, main event, displacement record. Time axis starts at 3:04:30 UTC.

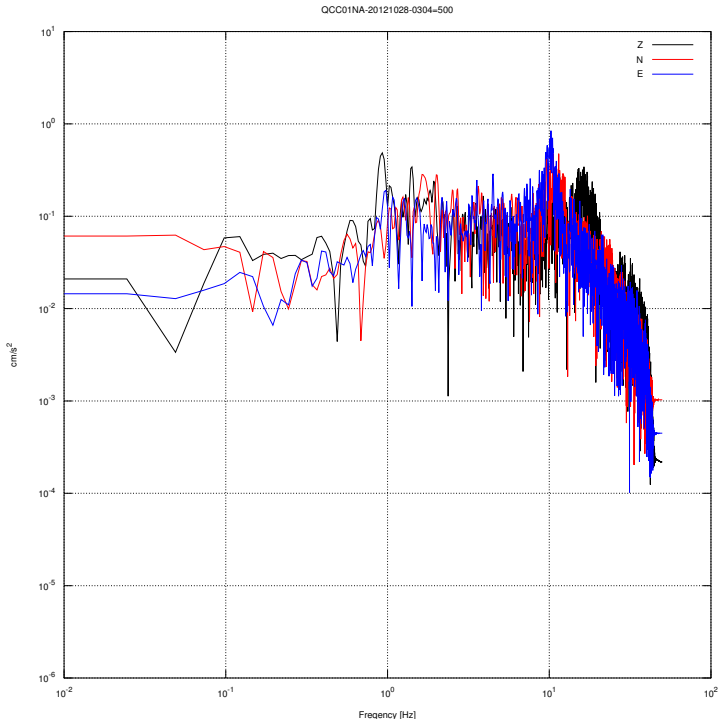

Figure 6: QCC01, main event, Fourier spectrum.

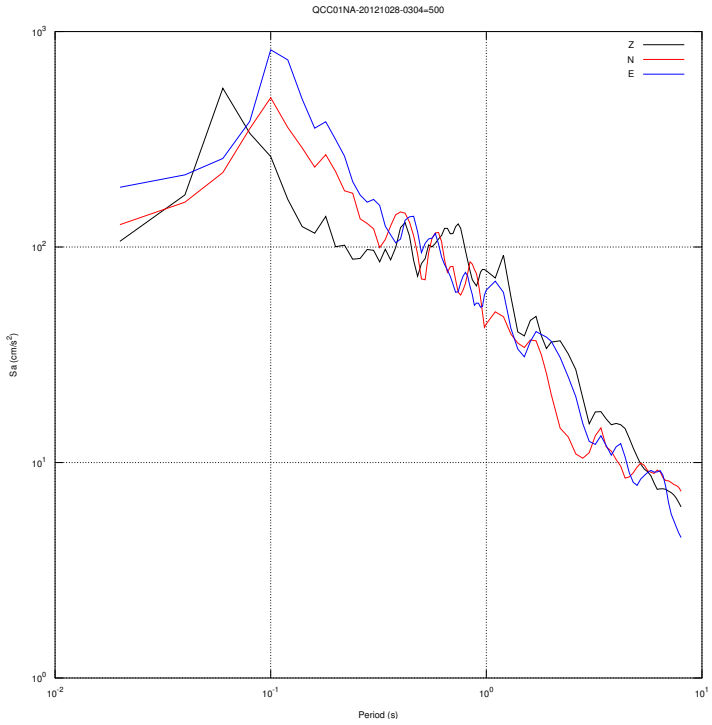

Figure 7: QCC01, main event, acceleration response spectrum, 5% damping.

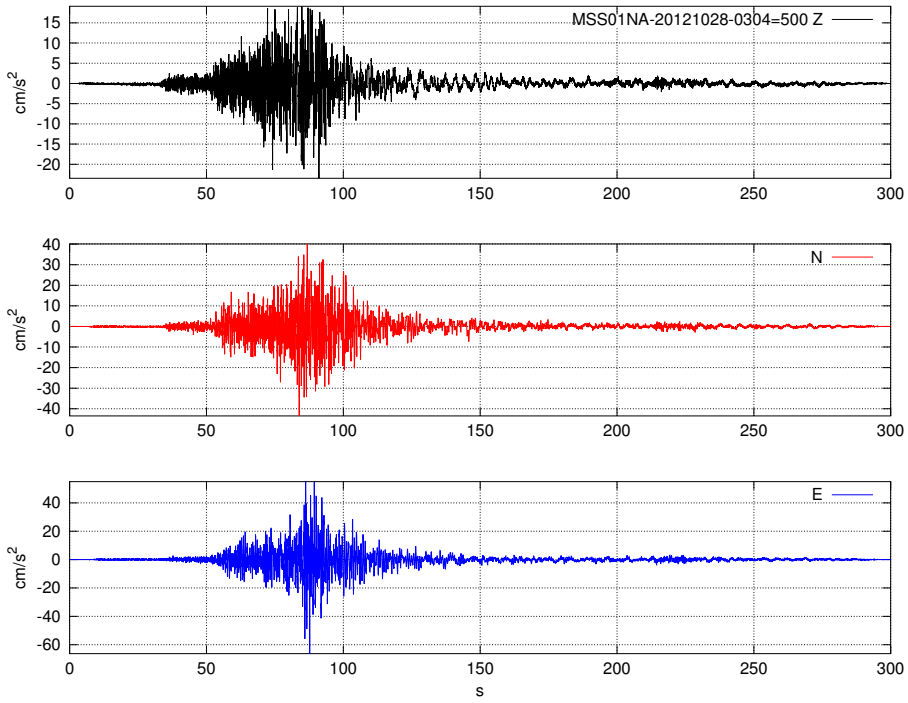

Figure 8: MSS01, main event, acceleration record. Time axis starts at 3:04:30 UTC.

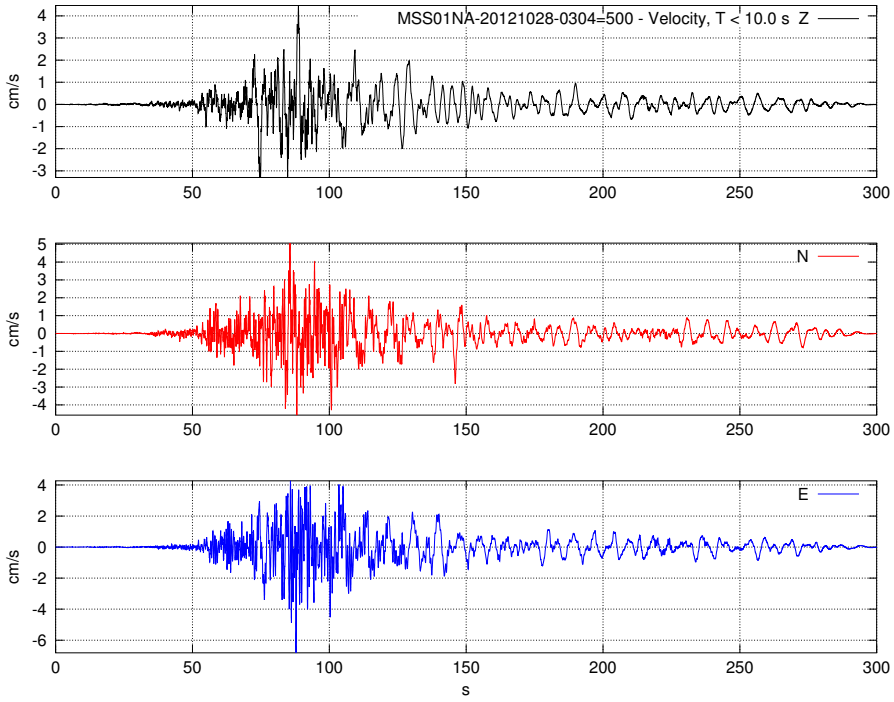

Figure 9: MSS01, main event, velocity record. Time axis starts at 3:04:30 UTC.

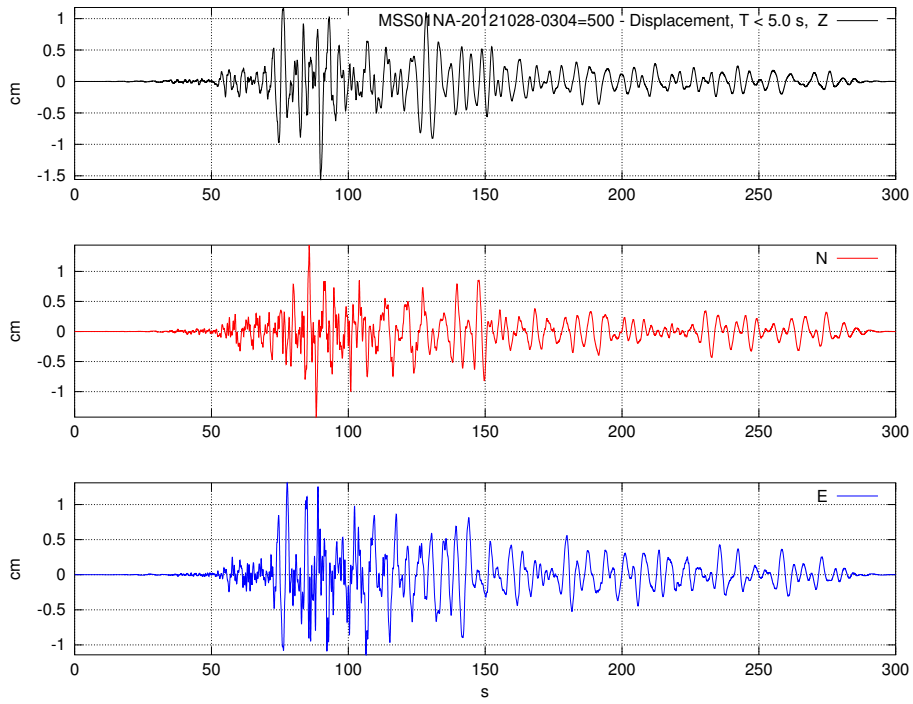

Figure 10: MSS01, main event, displacement record. Time axis starts at 3:04:30 UTC.

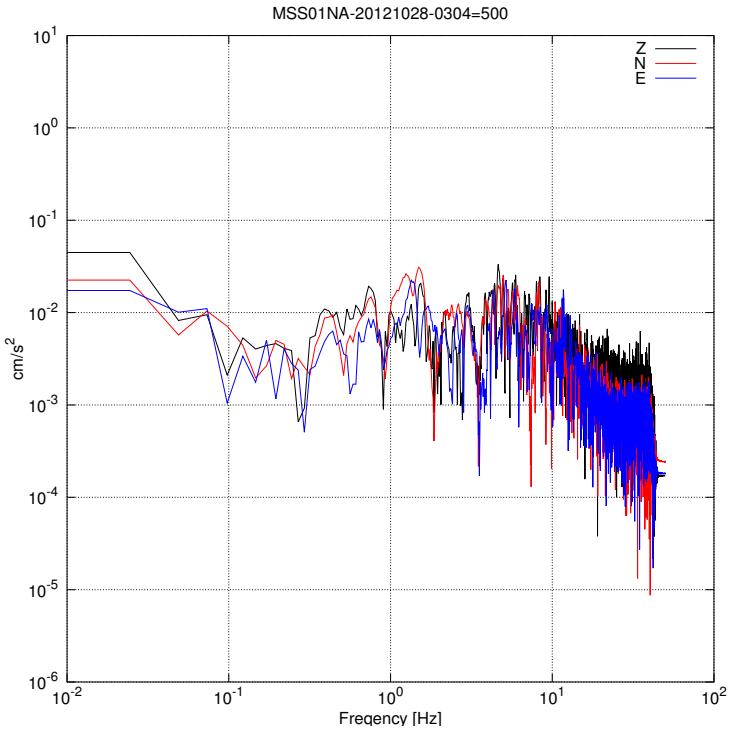

Figure 11: MSS01, main event, Fourier spectrum.

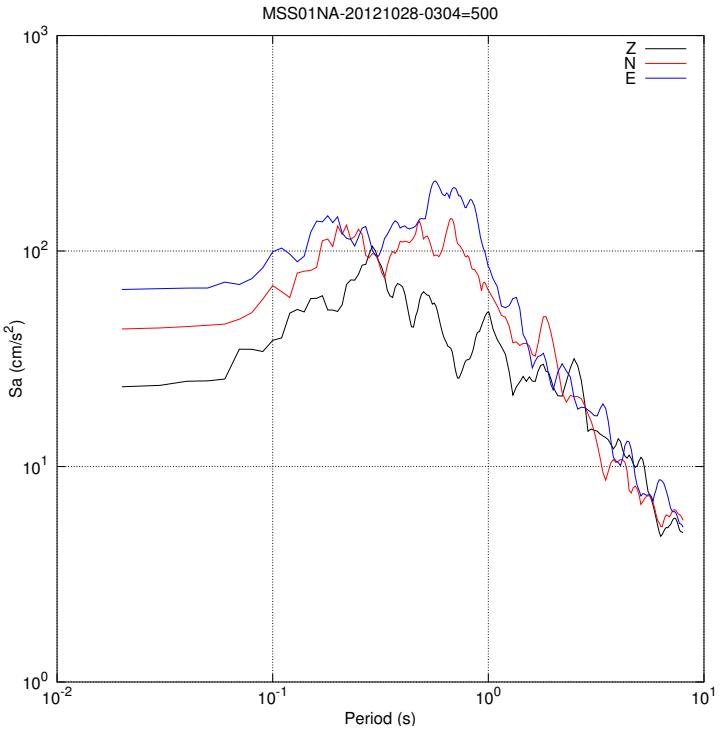

Figure 12: MSS01, main event, acceleration response spectrum, 5% damping.

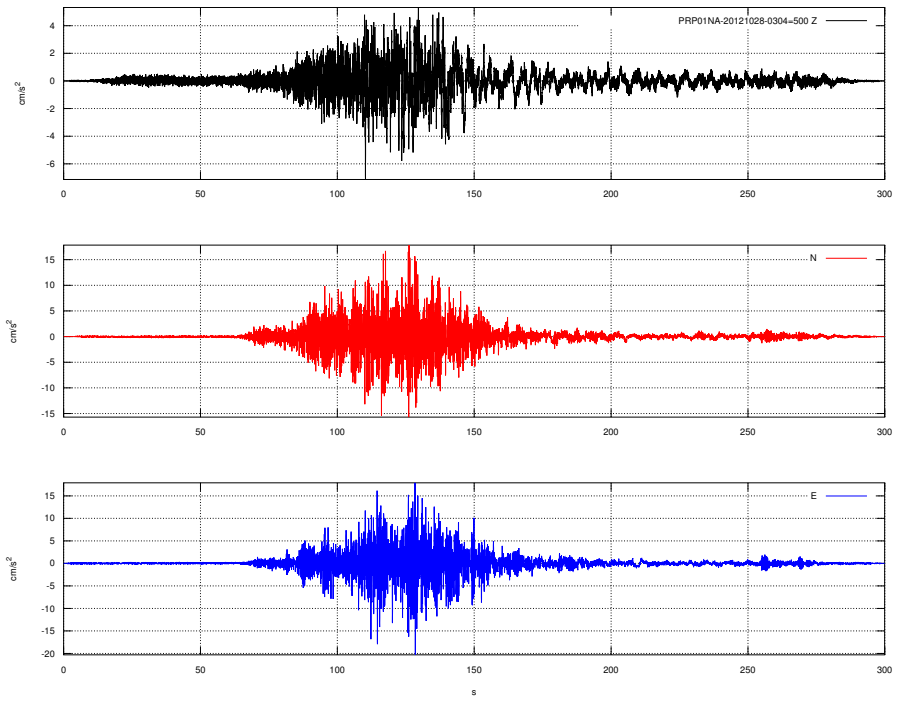

Figure 13: PRP01, main event, acceleration record. Time axis starts at 3:04:30 UTC.

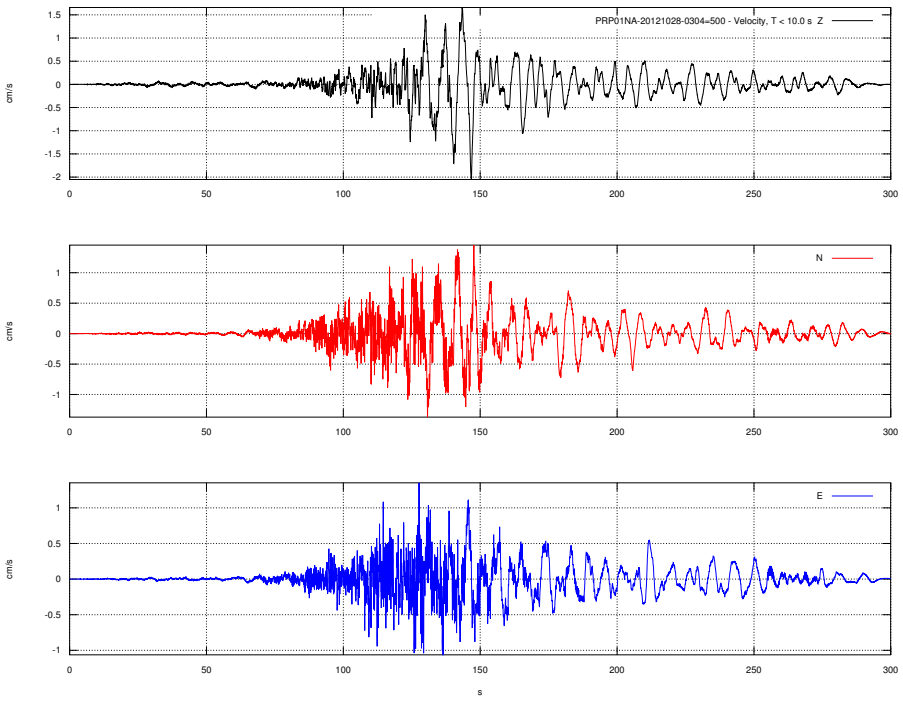

Figure 14: PRP01, main event, velocity record. Time axis starts at 3:04:30 UTC.

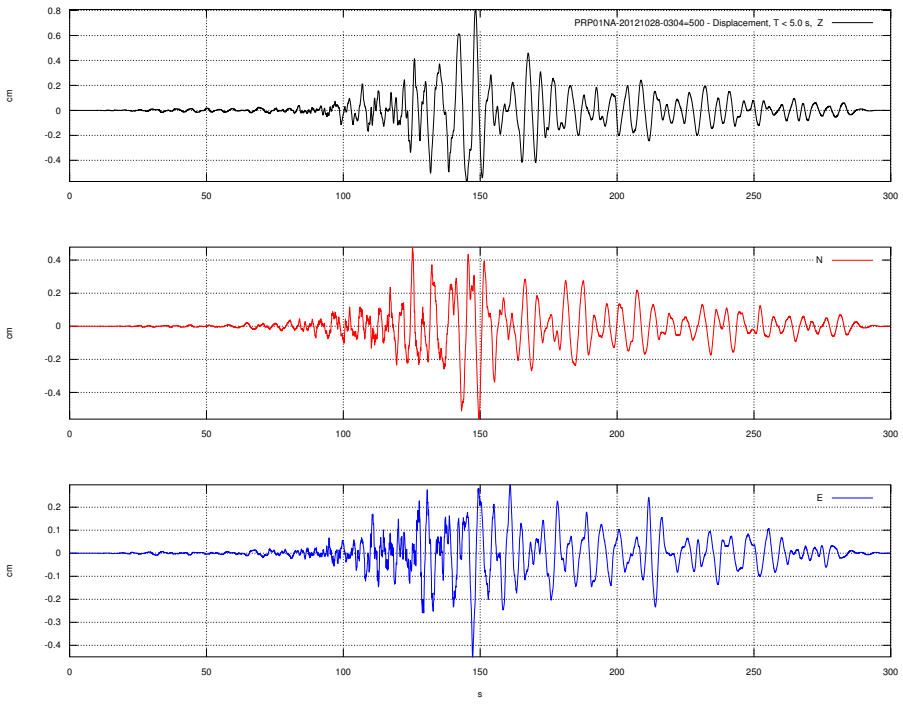

Figure 15: PRP01, main event, displacement record. Time axis starts at 3:04:30 UTC.

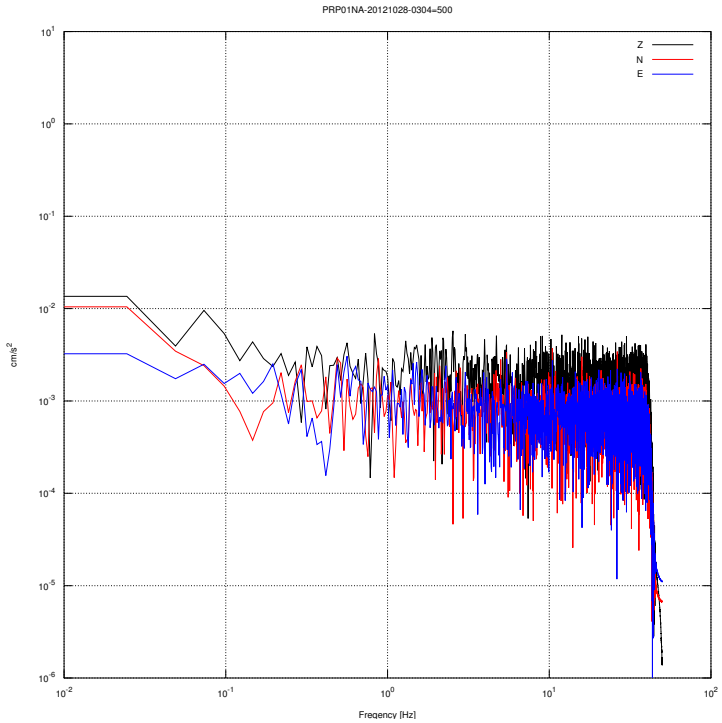

Figure 16: PRP01, main event, Fourier spectrum.

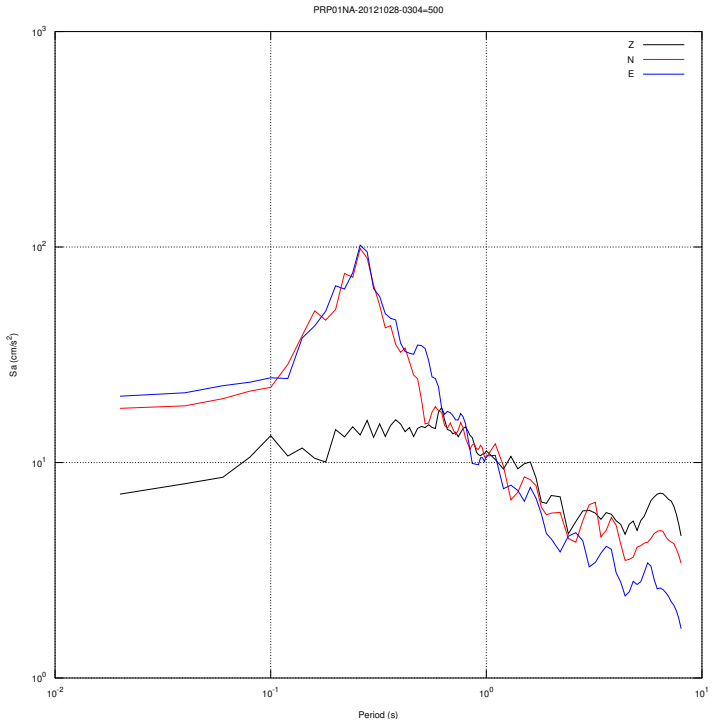

Figure 17: PRP01, main event, response spectrum, 5% damping.

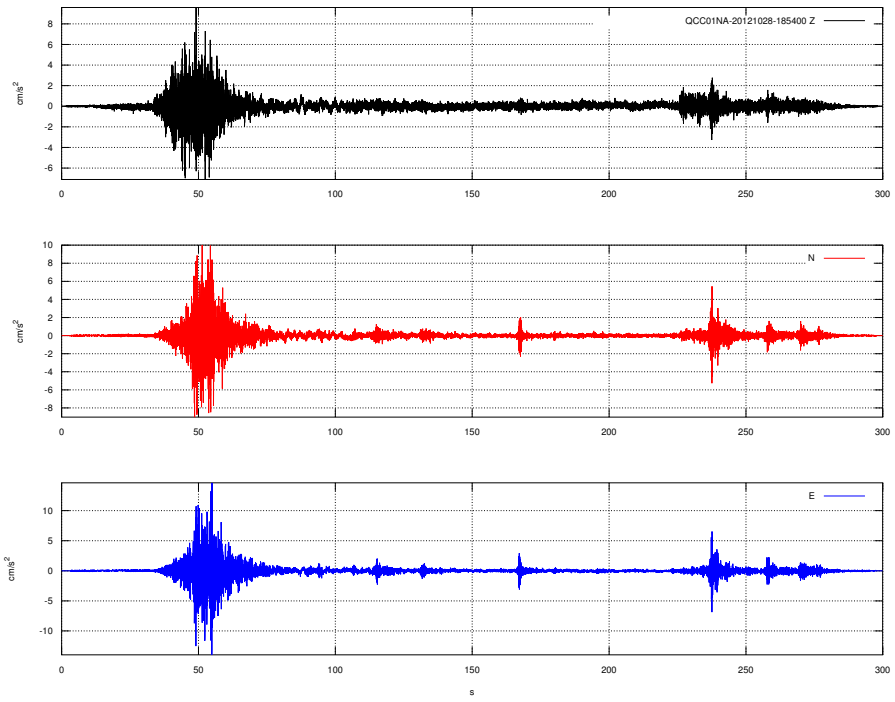

Figure 18: QCC01, Mw 6.3 aftershock, acceleration. Time axis starts at 18:54 UTC.

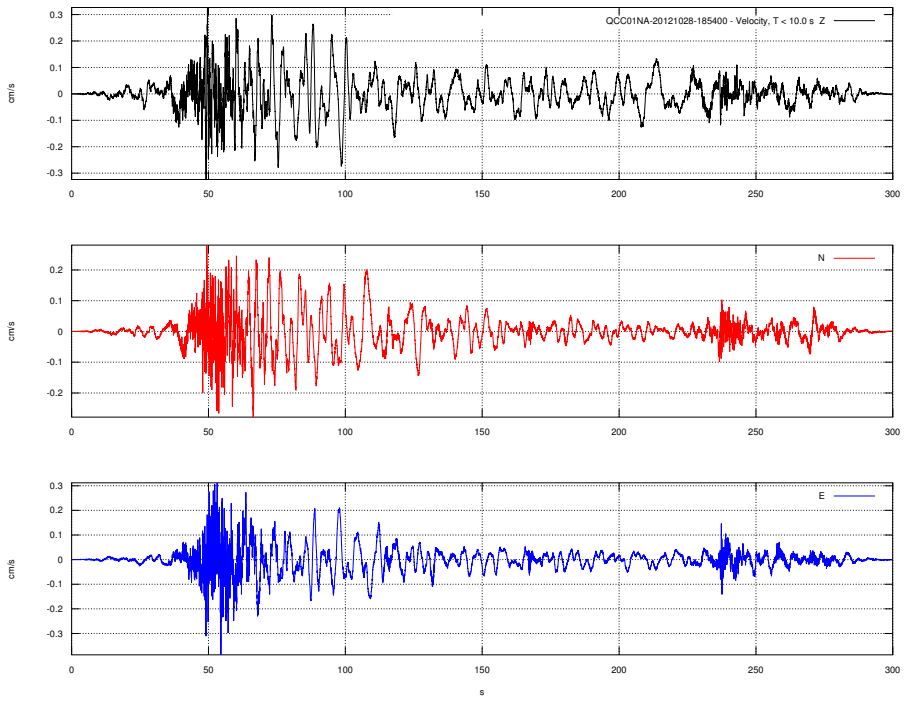

Figure 19: QCC01, Mw 6.3 aftershock, velocity. Time axis starts at 18:54 UTC.

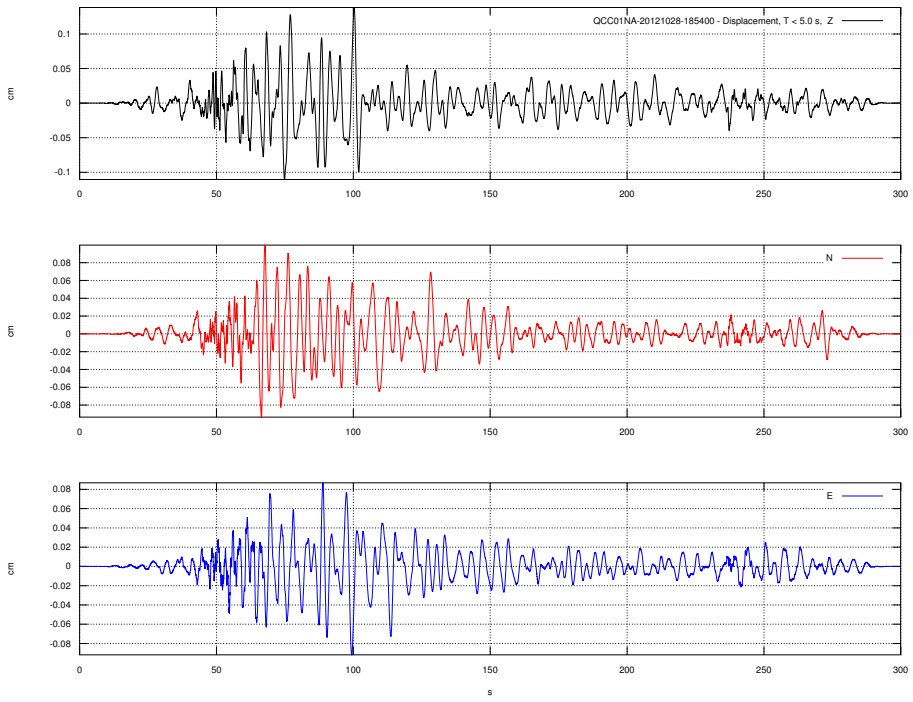

Figure 20: QCC01, Mw 6.3 aftershock, displacement. Time axis starts at 18:54 UTC.

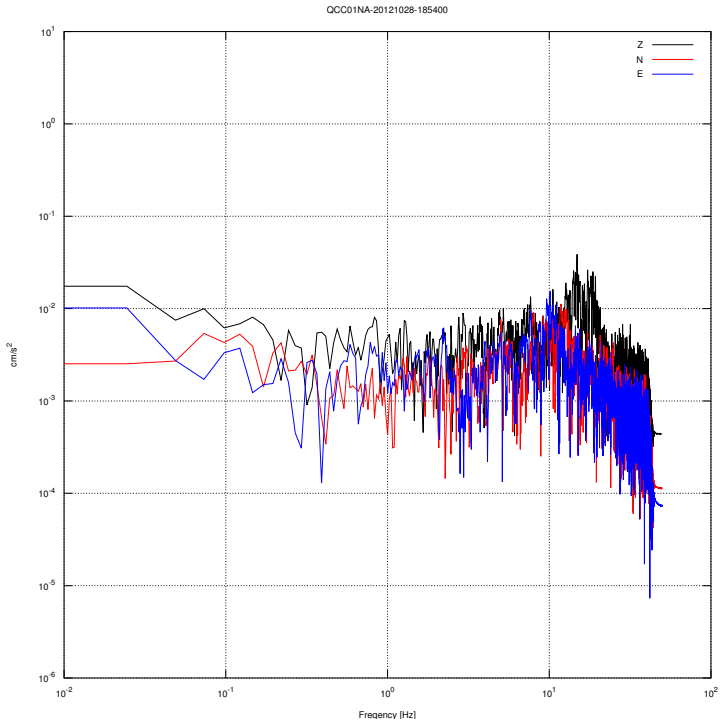

Figure 21: QCC01, Mw 6.3 aftershock, Fourier spectrum.

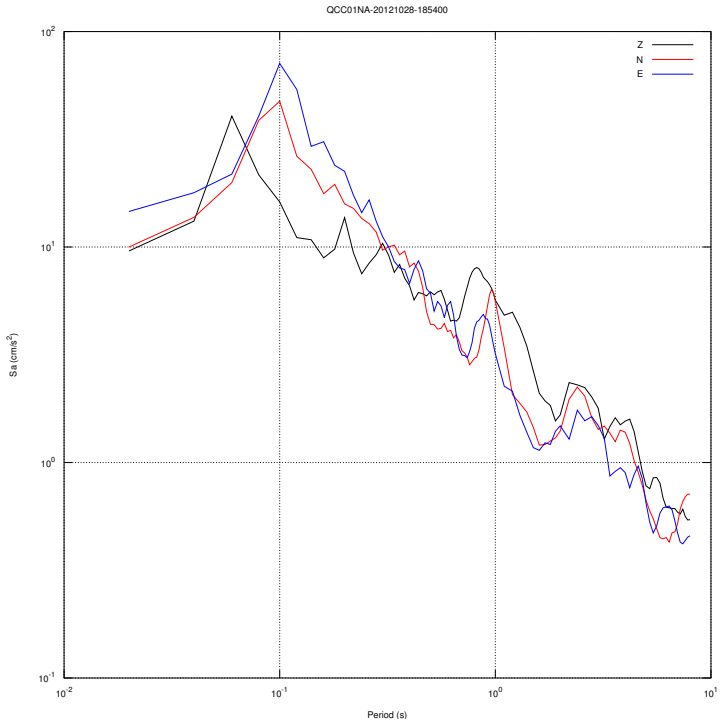

Figure 22: QCC01, Mw 6.3 aftershock, response spectrum, 5% damping.

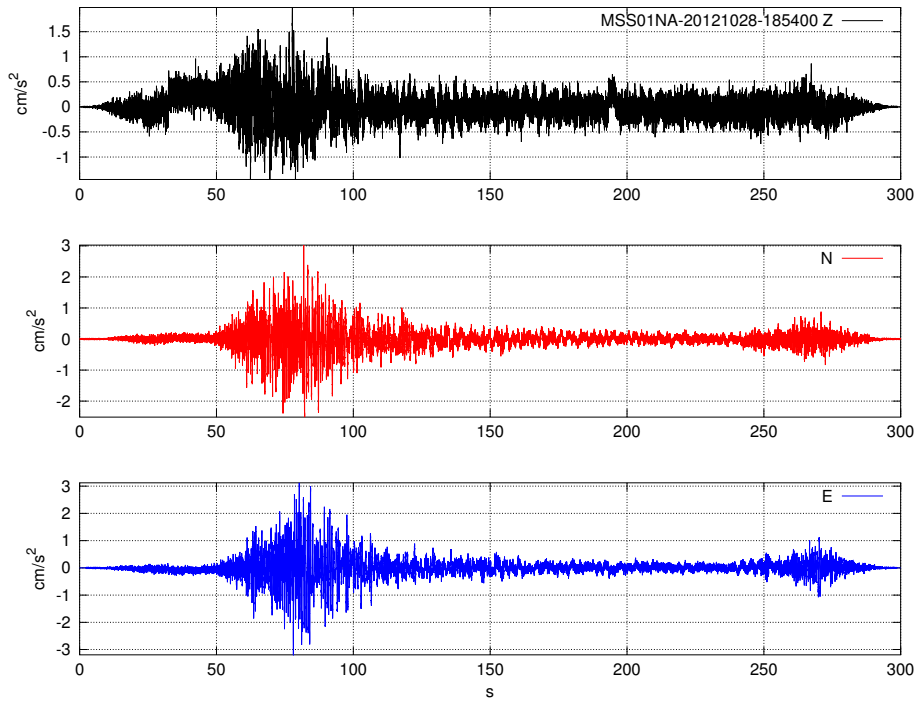

Figure 23: MSS01NA, Mw 6.3 aftershock, acceleration. Time axis starts at 18:54 UTC. The vertical component displays offset jumps at 30 and 190 seconds. The source of the interference is yet unknown.

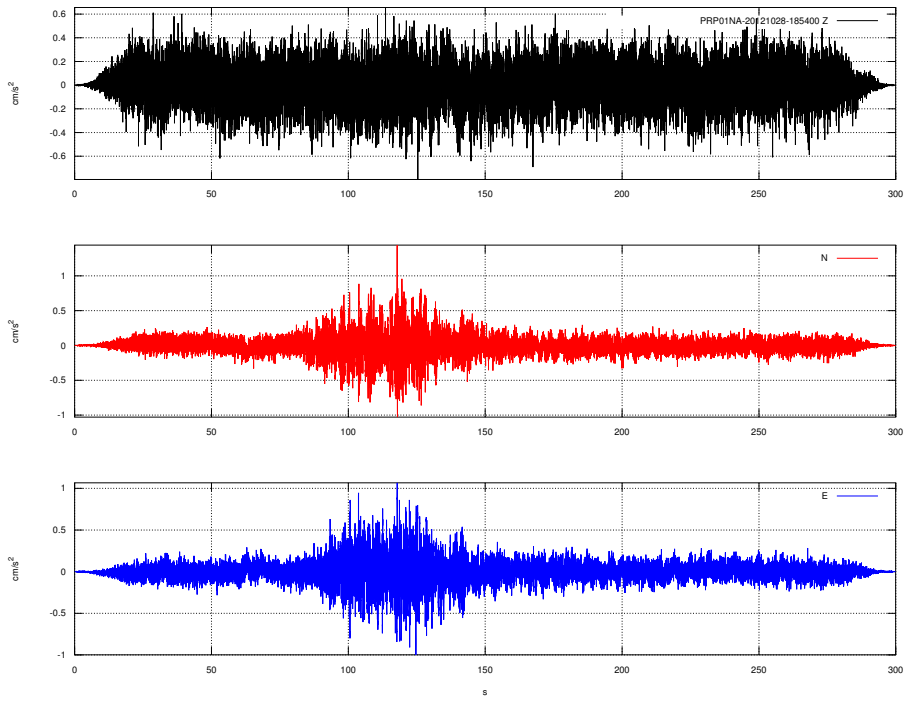

Figure 24: PRP01, Mw 6.3 aftershock, acceleration. Time axis starts at 18:54 UTC.

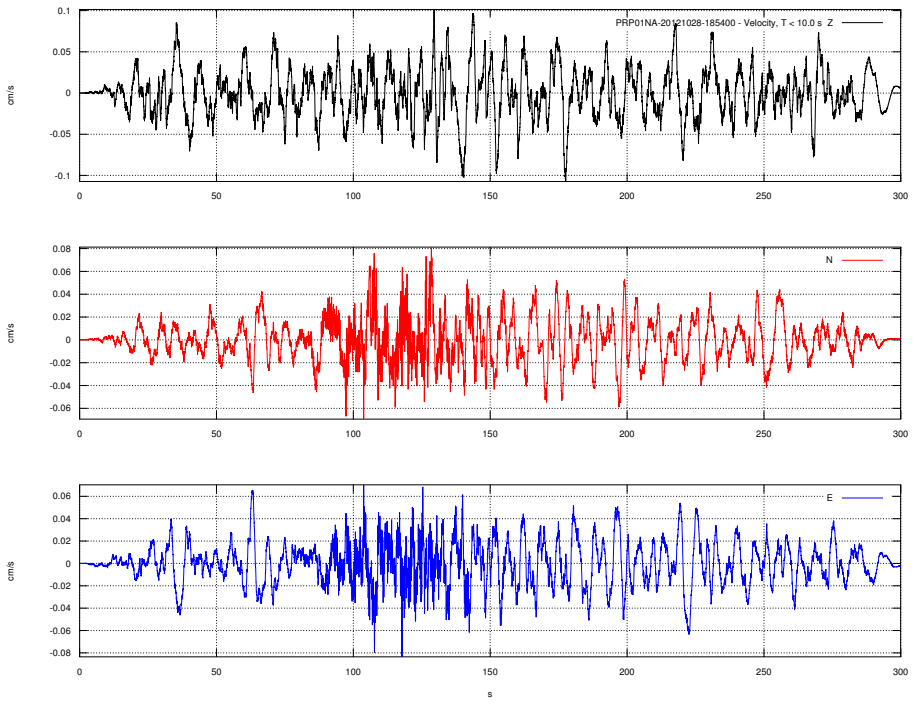

Figure 25: PRP01, Mw 6.3 aftershock, velocity. Time axis starts at 18:54 UTC.

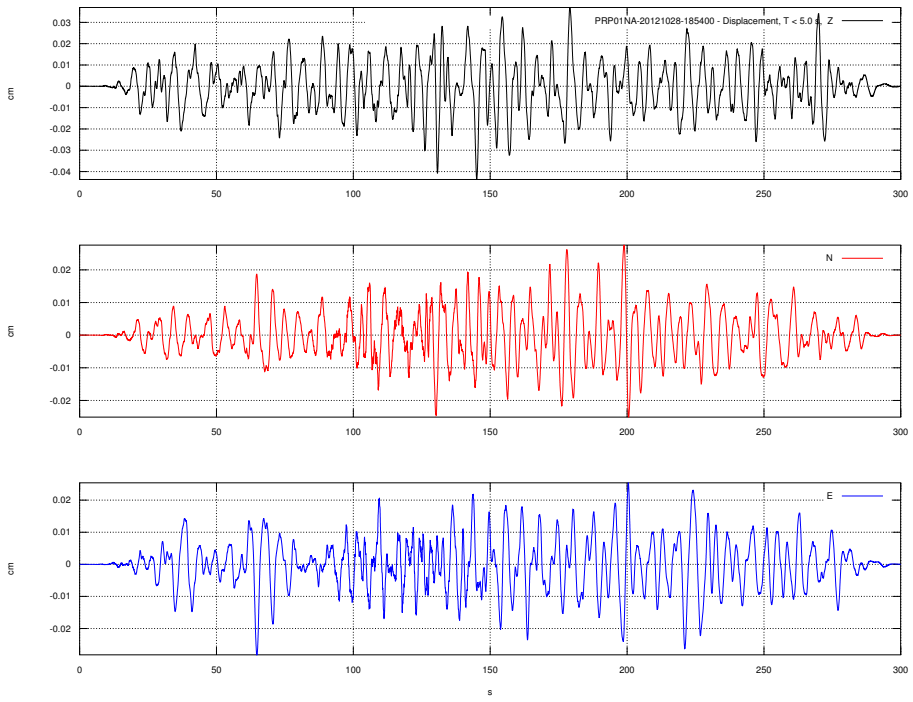

Figure 26: PRP01, Mw 6.3 aftershock, displacement. Time axis starts at 18:54 UTC.

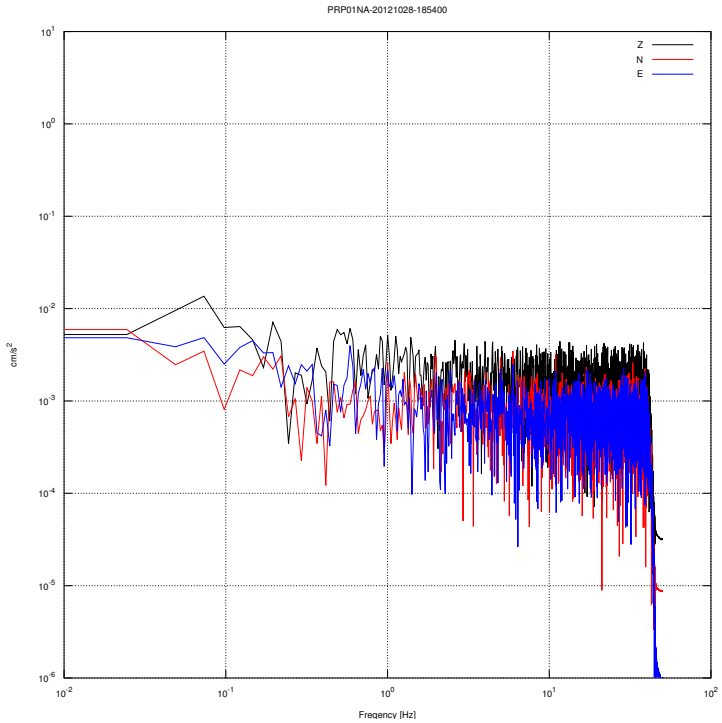

Figure 27: PRP01, Mw 6.3 aftershock, Fourier spectrum.

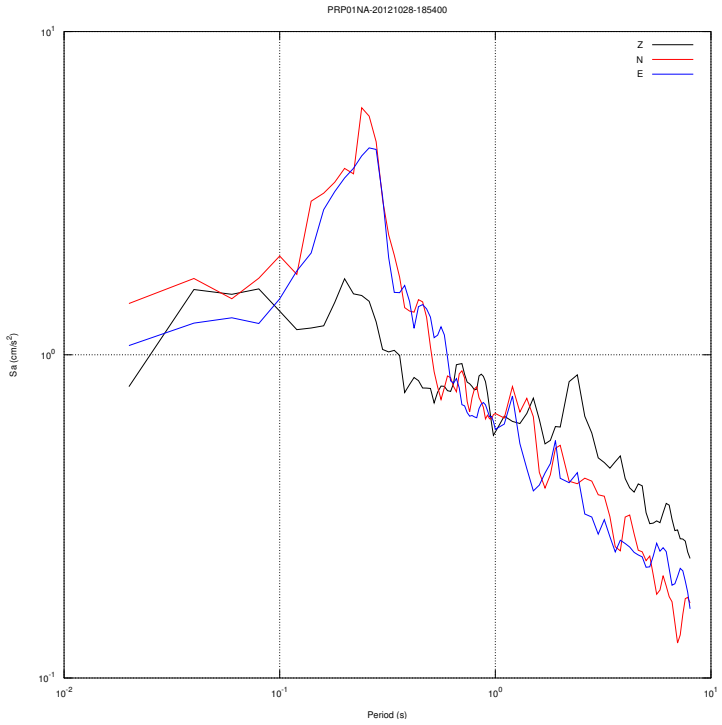

Figure 28: PRP01, Mw 6.3 aftershock, response spectrum, 5% damping.

References

Atkinson, G. M. and Boore, D. M. (2003). Empirical ground-motion relations for subduction-zone earthquakes and their application to cascadia and other regions. *BSSA*, 93(4):1703–1729.

Boore, D. and Atkinson, G. (2008). Ground-motion prediction equations for the average horizontal component of pga, pgv, and 510.0 s. *Earthquake Spectra*, 24:99–138.

Rosenberger, A., Rogers, G., and Huffman, S. (2006). Real-time ground motion from the new strong motion seismic network in British Columbia, Canada. In *First European Conference on Earthquake Engineering and Seismology, Geneva*. Paper 689 on CDROM.

Ventura, C. E., Kaya, Y., Yao, F., Huffmann, S., and Turek, M. E. (2012). Seismic structural health monitoring of bridges in British Columbia, Canada. In *15 WCCE Lisbon*.